JOURNAL OF CRUSTACEAN BIOLOGY, 19(4): 671-683, 1999

GILL-CLEANING MECHANISMS OF THE MUD LOBSTER *THALASSINA ANOMALA* (DECAPODA: THALASSINIDEA: THALASSINIDAE)

Zenon B. Batang and Hiroshi Suzuki

ABSTRACT

The gill-cleaning mechanisms of the mud lobster *Thalassina anomala* were examined. The gill complement consists of 12 arthrobranchs and 5 podobranchs, both having cylindrical flattened filaments. Morphological inference suggested passive gill-cleaning mechanisms involving various setal systems; multidenticulate setae (on scaphognathite, setobranch, distal epipod), pappose setae (on coxae, proximal epipod), serrate setae (short setal tufts on limb coxae), and plumose setae (on carapace fringe). Smooth setae were found on the thoracic epimeron (inner wall of the branchial chamber) and inner branchiostegal margin. Small lamellar protrusions on the pereiopodal arthrodium were noted bearing dense pappose setae. The multidenticulate scaphognathite and epipodal setae were serrate distally. The digitate scale setules of multidenticulate setobranch, epipodal, and scaphognathite setae shared similarities: (1) digitation pattern gradually changes distally from angular to linear, (2) proximal setules incline toward the base while distal setules incline toward the tip with overlapping inclinations in a transition zone, and (3) setule density increases distally on the setal shaft. The multidenticulate scaphognathite setae have a V-form spiral arrangement on the distal part of the shaft, which is atypical in decapods. Aquarium observations did not show active gill cleaning by thoracic limbs, but general body grooming and respiratory reversal were observed. The phyletic relationships of gill-cleaning mechanisms, with notes on branchial morphology, are discussed.

Grooming mechanisms vary among decapod taxa, and predominantly involve the third maxillipeds, pereiopods, or other setiferous thoracic processes which prevent fouling of body surfaces, cephalothoracic appendages, embryos, and gills (Bauer, 1975, 1977, 1978, 1979, 1981, 1989; Hindley and Alexander, 1978; Martin and Felgenhauer, 1986; Pohle, 1989a, b; Fleischer *et al.*, 1992; Nickell *et al.*, 1998; Suzuki and McLay, 1998). Grooming behaviors are closely related in function, but usually differ in structural morphology (Bauer, 1977, 1981, 1989). Grooming has been regarded as a conservative systematic character denoting phyletic affinity and adaptive value in decapods (Bauer, 1981, 1989; Martin and Felgenhauer, 1986; Suzuki and McLay, 1998). Most grooming structures are characterized by the presence of setal systems whose diverse forms and lesser-known functions invite further scrutiny (Jacques, 1989; Watling, 1989; Fleischer *et al.*, 1992; Felgenhauer, 1992).

The respiratory process in decapod crustaceans draws water into the branchial chamber and predisposes the gills to deleterious fouling by particulate debris and epizoites (Bauer, 1989, 1998). Fouling of gills may seriously affect respiration and ion regulation (Bauer, 1981, 1989; Martin and Felgenhauer, 1986). Therefore, decapods have evolved a variety of gill-cleaning mechanisms to counter fouling pressures. These mechanisms include setiferous thoracic epipods (penaeids, nephropids, palinurids, and brachyurans), pereiopods (carideans, stenopodids, thalassinids, and anomurans), epipod-setobranch complex (carideans) or setobranchs only (axiids and astacids), scaphognathite setae (atyid carideans), and branchiostegal setae (astacids) (Bauer, 1981, 1989, 1998; Suzuki and McLay, 1998). An antifouling function has also been attributed to the compound fringe setae on limb articles and carapace (Bauer, 1981, 1989). Respiratory reversal, or the back-flushing of respiratory water from the branchial chamber, has been similarly recognized as gill-cleaning activity in decapods (Bauer, 1989), while the newly reported phenomenon of "limb rocking" (Bauer, 1998) may have been overlooked in other species. Limb rocking refers to intentional agitation of limbs thus jostling the setobranchs and setiferous epipods in the crayfish *Procambarus clarkii* Girard, 1852 (see Bauer, 1998).

In the Thalassinida Burkenroad, 1981, gill-cleaning mechanisms are less well known relative to other reptant taxa, with few and scattered references to axiids, upogebiids, and callianassids (Martin and Felgenhauer, 1986;

Bauer, 1989; Nickell *et al.,* 1998). Pereiopodal gill brushing has been found in callianassids and upogebiids, and setobranchs in axiids. Though thalassinids generally exhibit uniform subterranean habit and burrow-adapted morphology (Scholtz and Richter, 1995), variations in gill form are well recognized (Nash *et al.,* 1984; Astall *et al.* 1997). The group has widespread geographic distribution ranging from deep-sea to supralittoral zones of mangrove swamps (Labadie and Palmer, 1996) and their cosmopolitan range has been attributed to their morphological and behavioral adaptability (Nickell *et al.,* 1998). Thalassinids undergo active bioturbation which can have substantial geochemical impact through the redistribution of nutrients, trace metals, and radionuclides (Whitehead *et al.,* 1988; Ziebis *et al.,* 1996). Their fossorial habit presupposes constant exposure to fouling pressures and hypoxia, though various respiratory adaptations of the group to hypoxic, or even anoxic, conditions have been noted in Astall *et al.* (1997). Antifouling implications of burrowing behavior has also been suggested (Bauer, 1989). The systematic position of thalassinids remains unsettled and the taxon has been formerly grouped with the Anomura (Martin and Abele, 1986) or excluded from them (Scholtz and Richter, 1995). Based on gill-cleaning and body-grooming characters, Bauer (1989) concluded a thalassinid origin of the anomurans.

The mud lobster *Thalassina anomala* Herbst, 1804, or mangrove lobster to some authors (Yunker and Scura, 1985; Pillai, 1990), inhabits the eulittoral and supralittoral zones of mangrove swamps in estuarine tropical shores (Pillai, 1990). The species is a deposit feeder which can stand prolonged emersion despite its subterranean habit. It usually creates complex burrow systems that can reach 2 m deep and forms conical mounds on the ground surface which can significantly alter substrate topography (Pillai, 1992). The biomechanics of its chelae has been studied in relation to feeding, digging, and aggressive encounters (Pillai, 1990).

Here, we present aspects of thalassinid grooming behavior by describing the gill-cleaning mechanisms of the mud lobster based on morphological inference and aquarium observations. Emphasis is given to the ultrastructure and distribution of setiferous processes which are conceivably involved in gill cleaning. A synthesis of thalassinid gill-cleaning mechanisms is subsequently discussed.

Materials and Methods

Mud lobsters were collected from mangrove swamps in Lomboc Island, Indonesia, and Amami-oshima, southern Japan, in March and May 1998, respectively, by excavating burrows. Specimens were preserved in 70% alcohol. Body size was expressed in carapace length (CL: dorsomedial distance between the tip of the rostrum and the posterior edge of the carapace). Following dissection of the branchial chamber by cutting off the branchiostegites, the position, structure, and branchial formula of the gills were noted. Gross morphological observations of the branchial chamber, using larger specimens (CL > 5.0 cm), were conducted by light microscope (Nikon SMZ-U) with camera lucida.

The ultrastructures of gill-cleaning processes were observed by scanning electron microscope (SEM). For SEM preparation, branchiostegites were cut off and the entire cephalothorax halved longitudinally. Samples were dehydrated in 2-h series of ethyl alcohol (EtOH: 80%, 90%, 95%, 100%, 100%), later replaced with 2 mixtures (1:1, 2:1) of tri-butyl alcohol (t-BuOH) and EtOH, and 2 final changes of absolute t-BuOH. Samples in absolute t-BuOH were refrigerated overnight after which they were freeze-dried (VFD-21 t-BuFreeze Dryer), mounted on aluminum stubs, and coated on gold-palladium complex using EIKO IB3 Ion Coater and viewed on SEM (Hitachi S-4100H).

Visual observation of live specimens in the laboratory was conducted to determine species-specific behavior of gill cleaning. Single specimens were placed in a glass aquarium filled with brackish water and graded sediments, predominantly white fine sands, to ensure visual clarity. The aquarium was aerated continuously and the specimen fed with commercial crustacean food. Observation was done 3–5 h daily within a week and all signs of body-grooming activities, as defined by Bauer (1981), were recorded. Gill nomenclature follows Astall *et al.* (1997) where gills assigned to a thoracic somite are labeled according to associated thoracic appendages. For brevity, maxillipeds 1–3 and pereiopods 1–5 are indicated by M1–M3 and P1–P5, respectively. The description of setal systems is based on Felgenhauer (1992) and Watling (1989).

Results

Branchial Morphology

The mud lobster *T. anomala* has paired arthrobranchs (anterior and posterior) articulating on the arthrodium of M2–P4 (Figs. 1B, 2, Table 1). Podobranchs arise singly from the coxae of M2–P3. Podobranchs are well developed on M2–P2, rudimentary on P3, and lost on P4. Setiferous epipods are present on M2–P4, increasing in length posteriorly, with the P4 epipod being twice as long as the M2 epipod. The setiferous epipods originate on the same base as the podobranchs (Fig. 2), both projecting posteriorly, and filling the ventral periphery of the branchial chamber.

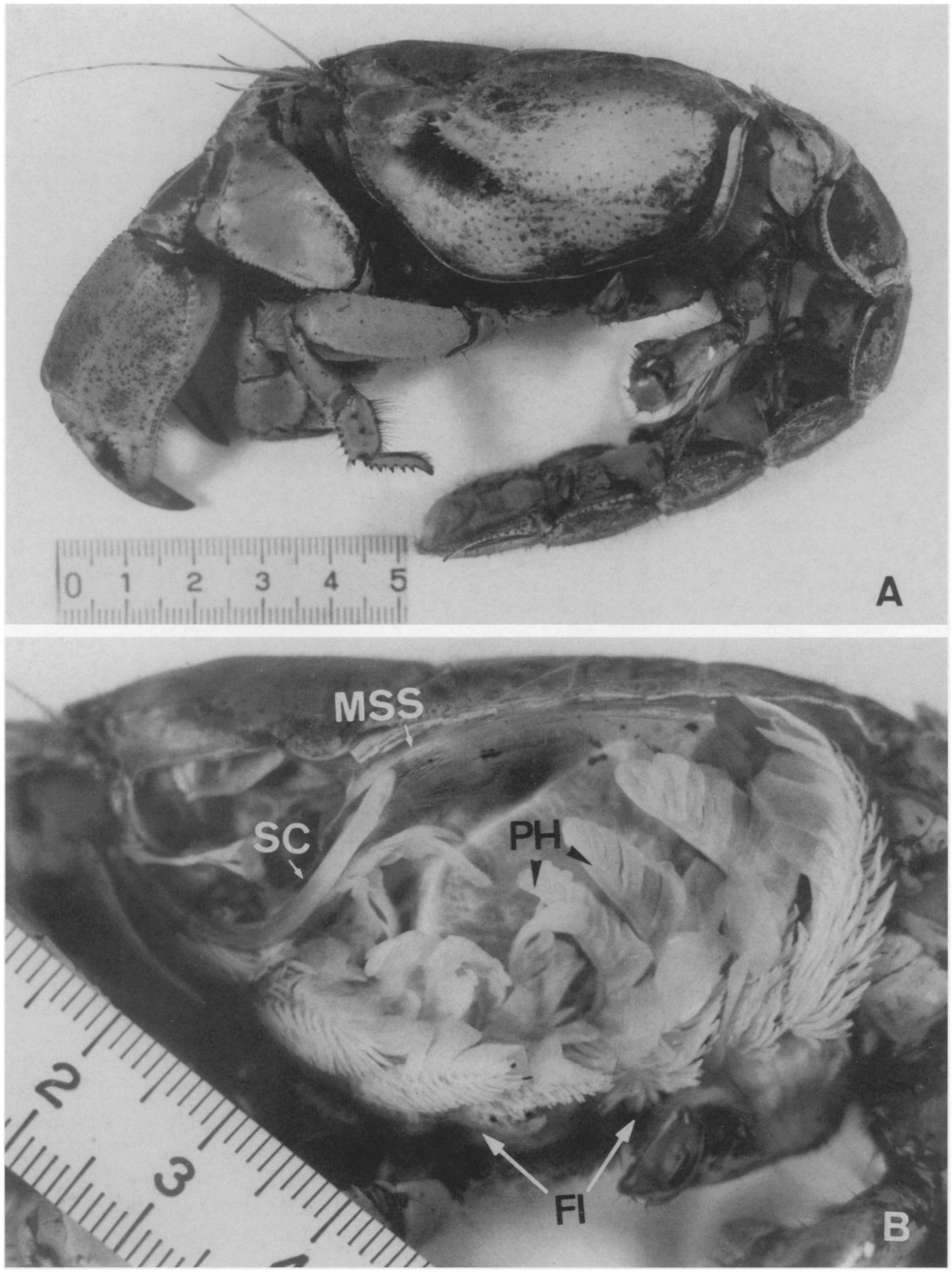

Fig. 1. *Thalassina anomala* Herbst, 1804. External (A) and internal (B) view of the branchial chamber showing phylloid (PH) and filamentous (FI) gills and the posterior edge of scaphognathite (SC) bearing long multidenticulate setae (MSS). Scale number in cm.

Overall, the mud lobster has 12 arthrobranchs and 5 podobranchs (rudimentary podobranch on P3 included) in the gill chamber. Pleurobranchs are lacking. Gills and an epipod are absent on P5.

The gills of *T. anomala* consist of two filament forms, cylindrical (filamentous type) and compressed (phylloid type) (Figs. 1B, 2). Both filament forms cooccur in all arthrobranchs and podobranchs. The phylloid fila-

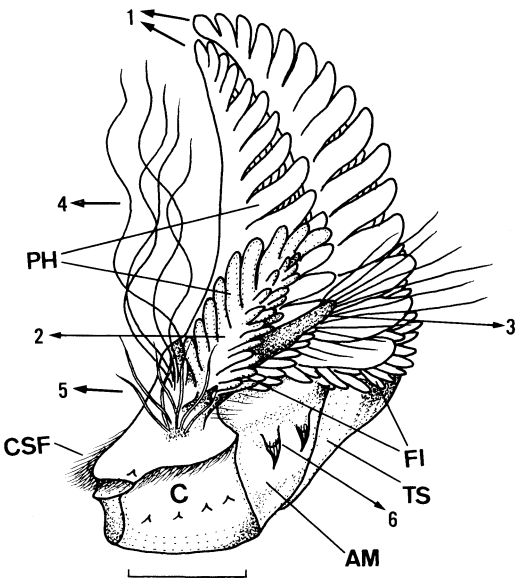

Fig. 2. Schematic diagram of the branchiae and setiferous processes associated with the second pereiopod of *Thalassina anomala* Herbst, 1804. Left is anterior part. 1, arthrobranchs (anterior and posterior); 2, podobranch; 3, epipod; 4, setobranch setae; 5, outer short coxal setae; 6, arthrodial lamellae bearing setae; PH-phylloid gill filaments; FI-filamentous gill filaments; TS-thoracic sternite; CSF-coxal setal fringe; C-coxa. Scale: 5 mm.

ments are longer but obviously have thinner cuticle than the filamentous filament. The latter filaments are enveloped in transparent epithelial sheaths. Within the branchial chamber, the phylloid filaments of arthrobranchs project upright, filling most of the branchial space, while the filamentous type protrude numerously on the basal section of the gill shaft and, together with the podobranchs, form stacks of filaments guarding the ventral periphery of the branchial chamber (Fig. 1B).

Gill-cleaning Processes and Setal Systems

Scaphognathite Setae.—A long scaphognathite arises from the second maxilla, extending posteriorly into the anterior branchial chamber (Fig. 1B). The posterior end of the scaphognathite is ornamented with long setae (Fig. 3A, B) bearing digitate scale setules (Fig. 3C). The multidenticulate scaphognathite setae (MSS), following Suzuki and McLay (1998), project from supracuticular sockets on the scaphognathite margins and extend as far as the phylloid filaments of P4 gills, which arch posteriorly following the marginal curvature of the branchial chamber. In addition, the dorsodistal margin of the tip of each scaphognathite bears four short smooth setae with hooked tips (Fig. 3B). Both setal types on the scaphognathite lack an annulus.

The scale setules of the MSS differ in digitation pattern and inclination along the setal shaft. The digitation pattern is angular proximally and gradually becomes linear on the distal part of the setal shaft. The angular digitate scales are randomly distributed on the proximal part of the setae and incline toward the setal base (Fig. 3E). The linear digitate scale setules become denser distally and incline toward the setal tip (Fig. 3F). The distal scale setules form V-shaped generative lines on the shaft, which appear to spiral at low magnification (Fig. 3C). The mixture of oppositely inclined scales (transition zone) generally occurs midlength along the setal shaft. The MSS taper and become serrated distally (Fig. 3D).

Coxal Setal Systems.—Four setal types arising on thoracic coxae are distinguished; long and short setal groups on the dorsolateral surface of the coxa, the setal fringe on coxal margins, and the setal tufts on arthrodial lamellae (Fig. 2).

The dorsolateral setae are found in two distinct locations on M3 and P1–P4, an inner group of long multidenticulate setae (Figs. 2, 4) and an outer group of short annulate serrate setae (Figs. 2, 5A–F). Both setal groups lie close to the epipodal base, with decreasing setal density posteriorly. The coxal surfaces do not show prominent papillar or tubercular formation, or setobranchs in the sense of Borradaile (1907), which abound in carideans and astacids (Bauer, 1981, 1998). By virtue of their morphology and location, we term the long multidenticulate setae "setobranch setae." These setobranch setae insert into gill filaments (Figs. 4A, 6A) and their digitate scale setules imply a gill-cleaning function (Bauer, 1981, 1998). The setae arise from basal sockets on the coxa (Fig. 4-1), thus allowing them to move flexibly when jostled. The digitate scale setules of the setobranch setae also vary in shape and orientation along the shaft (Fig. 4). One twentieth of the setal length from the base is naked and without an annulus (Fig. 4-1), after which scale setules appear and incline proximally (Fig. 4-2). A transition zone of setule inclination spans a region nearly equal to one-fifth

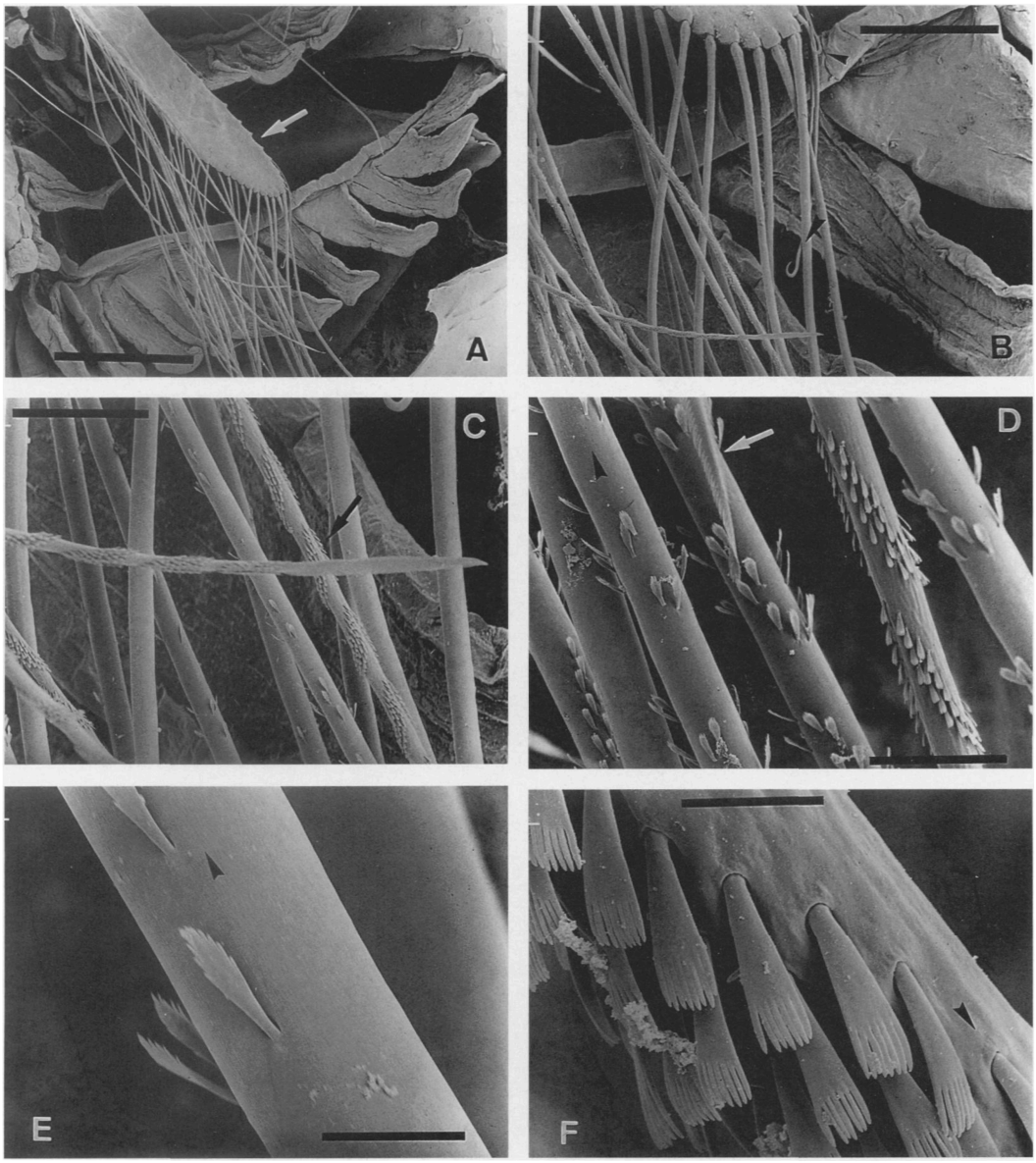

Fig. 3. *Thalassina anomala* Herbst, 1804. A, posterior edge of scaphognathite (arrow) with multidenticulate setae; B, proximal view of multidenticulate scaphognathite setae (MSS) and smooth setae with hooked tips (arrowheads); C, V-form arrangement of scale setules on distal part of MSS showing spiral appearance (black arrow); D, MSS scale setules and serrate tip (white arrow); E, proximal scale setules of MSS showing digitation pattern (angular type) and inclination (arrowhead points to base of seta); F, distal MSS scale setules with linear digitation pattern and inclination to setal tip (arrowhead points to tip of seta). Scale bars: A = 749 μm; B = 231 μm; C = 86 μm; D = 43 μm; E = 10 μm; F = 4 μm.

of the setal shaft (Fig. 4-3 to 4-5), thereafter the scale setules incline distally until the setal tip (Fig. 4-6 to 4-8). Setule density increases from base to tip.

The outer short setae (Fig. 5A) are serrate and project from cuticular sockets (Fig. 5B) on the coxal surface. The proximal part of the seta is naked (Fig. 5C) and bears an annulus (Fig. 5D), followed by a linear series of spiniform serrules which is interrupted by a short naked trunk halfway along the length (Fig. 5E). The spiniform serrules branch out in two opposite generative lines along the shaft and are oriented toward the setal tip (Fig. 5F). The

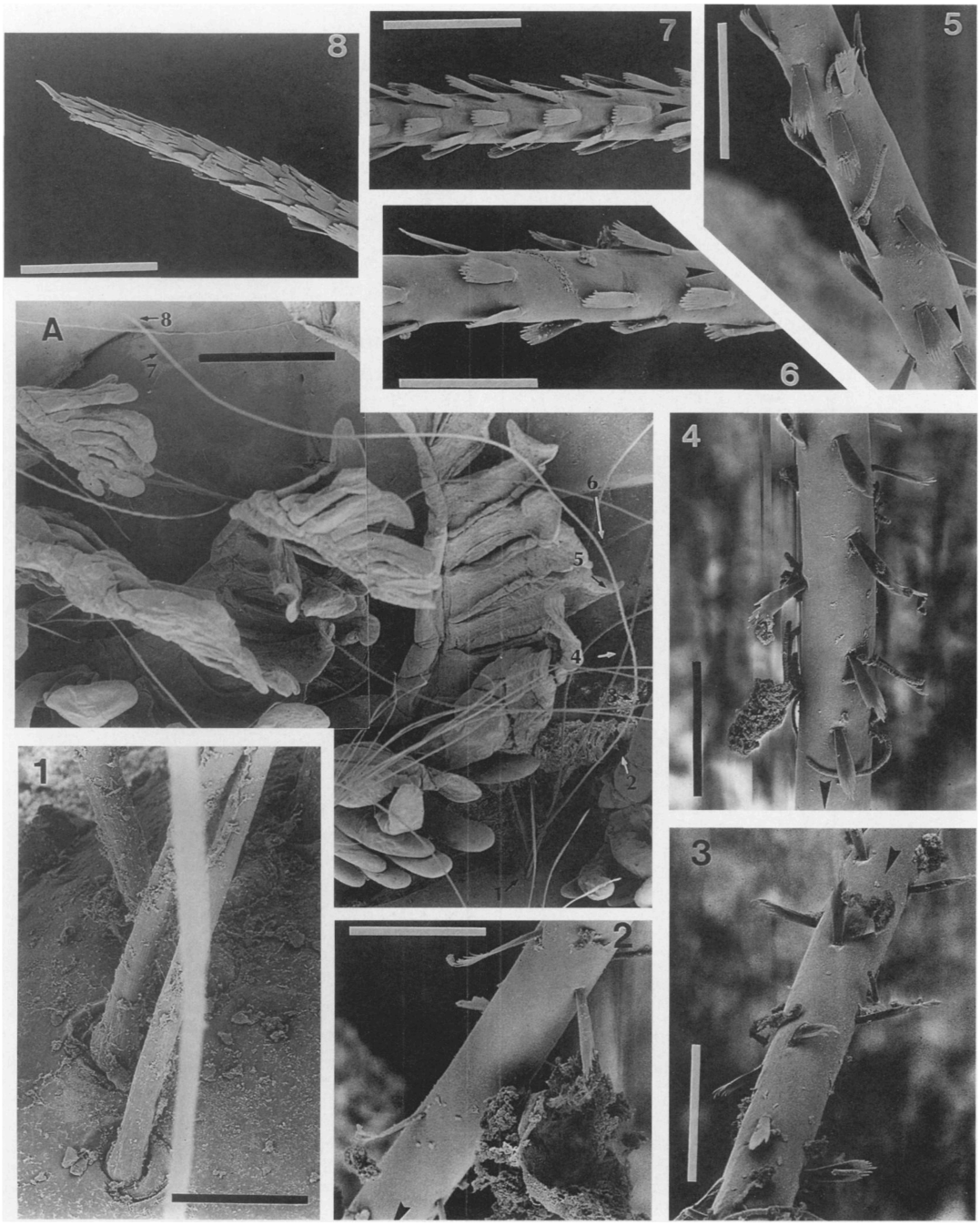

Fig. 4. *Thalassina anomala* Herbst, 1804. A, multidenticulate setobranch setae on coxa, with magnified sections (1–8) of setal shaft. Arrows point to approximate position of magnified sections. Arrowheads in 2–7 point toward base of seta. Scale bars: A = 784 μm; 1 = 70 μm; 2–4 = 23 μm; 5, 6 = 22 μm; 7, 8 = 20 μm.

→

Fig. 5. *Thalassina anomala* Herbst, 1804. A, outer tuft of serrate setae on coxa (arrowhead) of fourth pereiopod. Note small lobular protrusion (white arrow), gill filaments (GF) of arthrobranch, and proximal pappose setae (PS) on basal part of epipod (E); B, C, base of serrate setae showing naked proximal part and sockets; D, annulus (arrow); E, naked trunk interrupting serrate part; F, spiniform serrules on distal part of seta. Scale bars: A = 737 μm; B = 230 μm; C = 120 μm; D = 23 μm; E = 59 μm; F = 22 μm.

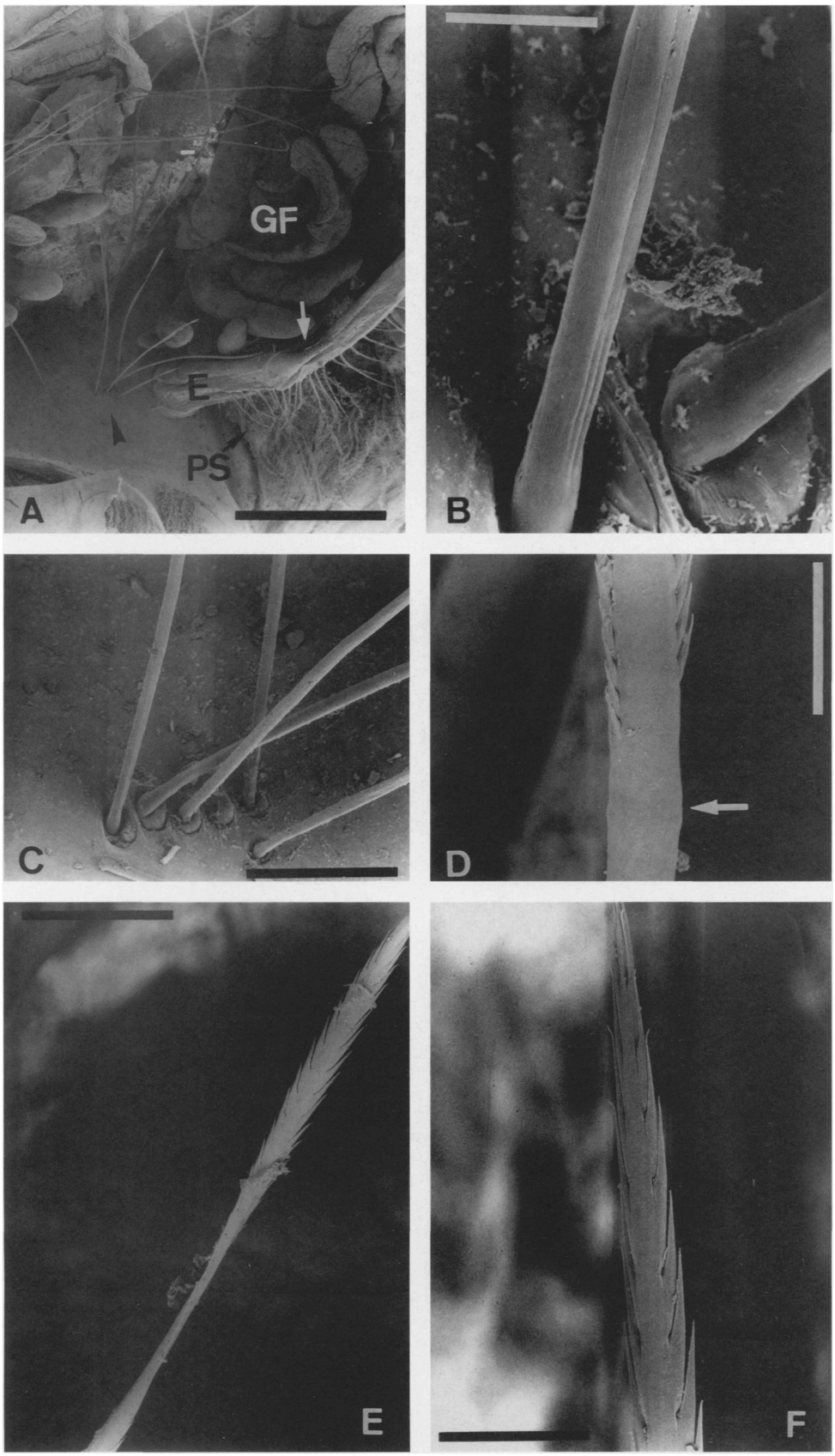
GF
E
PS
A
B
C
D
E
F